JPET Fast Forward. Published on July 3, 2019 as DOI: 10.1124/jpet.119.259895
This article has not been copyedited and formatted. The final version may differ from this version.

JPET # 259895

Oral Phenelzine Treatment Mitigates Metabolic Disturbances in Mice Fed a High-Fat Diet

JPET Fast Forward. Published on July 3, 2019 as DOI: 10.1124/jpet.119.259895
This article has not been copyedited and formatted. The final version may differ from this version.

JPET # 259895

Running title: Phenelzine mitigates HFD-derived metabolic disturbances

Josep Mercader[1,2]*, Agustín G Sabater[3], Sophie Le Gonidec[4,5], Pauline Decaunes[4,5], Alice Chaplin[6], Saioa Gómez-Zorita[7,8], Fermín I Milagro[8,9], Christian Carpéné[4,5]*

[1] Balearic Islands Health Research Institute (IdISBa), Palma de Mallorca, Spain; josep.mercader@uib.es

[2] Department of Fundamental Biology and Health Sciences, University of the Balearic Islands (UIB), Palma de Mallorca, Spain

[3] Alimentómica, S.L., Spin-off from the UIB, Palma de Mallorca, Spain

[4] Institute of Metabolic and Cardiovascular Diseases, INSERM, UMR1048, Team 1, 31342 Toulouse, France; christian.carpene@inserm.fr

[5] I2MC, University of Toulouse, UMR1048, Paul Sabatier University, 31432 Toulouse Cedex 4, France

[6] Cardiovascular Research Institute, School of Medicine, Case Western Reserve University, Cleveland, OH 44106; amc315@case.edu

[7] Nutrition and Obesity Group. Department of Nutrition and Food Science, University of the Basque Country (UPV/EHU) and Lucio Lascaray Research Institute, Vitoria, Spain; saioa.gomez@ehu.eus

[8] CIBERobn Physiopathology of Obesity and Nutrition, Institute of Health Carlos III, Spain

[9] Department of Nutrition, Food Science and Physiology; Centre for Nutrition Research, University of Navarra, Pamplona, Spain

* Correspondence: josep.mercader@uib.es ; christian.carpene@inserm.fr

Number of text pages: 36

Number of tables: 2

Number of figures: 8

Number of references: 64

Number of words in the abstract: 223

Number of words in the introduction: 631

Number of words in the discussion: 1453

List of non-standard abbreviations:

amine oxidase copper containing 3 (AOC3); carnitine palmitoyltransferase 1B (CPT1B); cluster of differentiation 36 (CD36); cluster of differentiation 45 (CD45); glucose transporter 4 (GLUT4); homeostatic model assessment of insulin resistance (HOMA-IR);

JPET Fast Forward. Published on July 3, 2019 as DOI: 10.1124/jpet.119.259895
This article has not been copyedited and formatted. The final version may differ from this version.

hormone-sensitive lipase (HSL)

inguinal white adipose tissue (iWAT); interscapular brown adipose tissue (iBAT); monocyte chemoattractant protein 1 (MCP1); non-esterified fatty acids (NEFA); oral glucose tolerance test (OGTT); peroxisome proliferator activated receptor alpha (PPARA); peroxisome proliferator-activated receptor gamma coactivator 1-alpha (PPARGC1A); phosphoenolpyruvate carboxykinase (PEPCK); quantitative insulin sensitivity check index (QUICKI); perirenal plus retroperitoneal white adipose tissue (pWAT); revised quantitative insulin sensitivity check index (R-QUICKI); scavenger receptor class B type 1 (SR-B1); semicarbazide-sensitive amine oxidase (SSAO); sterol regulatory element-binding protein-1c (SREBP1c); tumor necrosis factor (TNF); uncoupling protein 1 (UCP1); uncoupling protein 3 (UCP3) ; vascular adhesion protein-1 (VAP-1); vascular endothelial growth factor (VEGF).

Abstract

Novel mechanisms and health benefits have been recently suggested for the antidepressant drug phenelzine, known as a non-selective (MAO) inhibitor. They include an anti-lipogenic action that could have an impact on excessive fat accumulation and obesity-related metabolic alterations. We evaluated the metabolic effects of an oral phenelzine treatment on mice fed a high-fat diet (HFD). Eleven-week-old male C57BL/6 mice were fed a HFD and either a 0.028% phenelzine solution (HFD+PHE) or water to drink for 11 weeks. Phenelzine attenuated the increase in body weight and adiposity without affecting food consumption. Energy efficiency was lower in HFD+PHE mice. Lipid content was reduced in subcutaneous fat pads, liver and skeletal muscle. In white adipose tissue (WAT), phenelzine reduced sterol regulatory element-binding protein-1c and phosphoenolpyruvate carboxykinase mRNA levels, inhibited amine-induced lipogenesis, and did not increase lipolysis. Moreover, HFD+PHE mice presented diminished levels of hydrogen peroxide release in subcutaneous WAT, and reduced expression of leukocyte transmigration markers and pro-inflammatory cytokines in visceral WAT and liver. Phenelzine reduced the circulating levels of glycerol, triacylglycerols, HDL-cholesterol and insulin. Insulin resistance was reduced, without affecting glucose levels and glucose tolerance. On the other hand, phenelzine increased rectal temperature and slightly increased energy expenditure. The mitigation of HFD-induced metabolic disturbances points towards a promising role for phenelzine in obesity treatment and encourages further research on its mechanisms of action.

Significance statement:

Phenelzine reduces body fat, markers of oxidative stress, inflammation and insulin resistance in HFD mice. SSAO, MAO, PEPCK and SREBP1c are involved in the metabolic effects of phenelzine. Phenelzine could be potentially used for the treatment of obesity-related complications.

Introduction

Phenelzine (β-phenylethylhydrazine) is a nonselective MAO inhibitor prescribed to treat depression and anxiety disorder, which has been superseded by novel drugs, partly due to its side effects, which include hypertensive crisis, hypoglycaemia, food cravings and body weight gain. However, it is thought that phenelzine is not used proportionally to its benefits to adverse effects ratio. Benefits include a neuroprotective role, which has been demonstrated after the identification of novel phenelzine targets (reviewed in (Song et al., 2013; Baker et al., 2019)), including the chemical sequestration of reactive aldehydes in a manner that seems to be related to the hydrazine structure of phenelzine (Baker et al., 2019). Moreover, phenelzine also inhibits histone lysine-specific demethylases and may play a role in epigenetic regulations (Yan et al., 2016). On the other hand, the adverse effects have been reconsidered because the risk of hypertensive crisis associated with concomitant high tyramine dietary intake is lower than initially expected. Increased food intake and body weight are unwanted effects reported for many other psychotropic drugs (Zimmermann et al., 2003), such as olanzapine, which impairs lipolysis in adipocytes (Minet-Ringuet et al., 2007). However, in the case of phenelzine, studies have suggested an anti-obesity potential (reviewed in (Carpéné et al., 2019)), which reinforce the idea that weight gain could be a consequence of the improvement of psychiatric disorders rather than a direct effect (Zimmermann et al., 2003).

Phenelzine's anti-obesity potential is attributed to an impairment of lipogenesis (Carpéné et al., 2019). We recently reported that chronic phenelzine treatment reduces body fat in normal-weight mice without cardiovascular impairment (Carpéné et al., 2018c). Reduced body weight has been observed in a genetic obesity model (Carpéné et al., 2008). This effect was partly attributed to an inhibition of primary amine oxidase, also called semicarbazide-sensitive amine oxidase and vascular adhesion protein-1 (SSAO/VAP-1), a membrane-bound protein abundant in adipocytes involved in the aetiology of metabolic and cardiovascular diseases (Pannecoeck et al., 2015). The reduction in fat deposition by semicarbazide administration and SSAO activity (Mercader et al., 2011), implies a reduction in the subsequent hydrogen peroxide (H_2O_2) production that acts as an insulin-mimetic compound in adipocytes (Zorzano et al., 2003). Accordingly, the anti-lipogenic action of SSAO inhibitors has been demonstrated (Carpéné et al., 2008; Carpéné et al., 2013), whereas SSAO substrates enhance glucose transport and lipogenesis via increased H_2O_2 in adipocytes (Morin et al., 2001; Zorzano et al., 2003; Iglesias-Osma et al., 2004), and thus have been proposed as a treatment

option for diabetes (Mercader et al., 2010). The phenelzine inhibitory effect on lipid accumulation might involve SSAO-independent targets, including sterol regulatory element-binding protein-1c (SREBP1c) (Chiche et al., 2009) and phosphoenolpyruvate carboxykinase (PEPCK) (Carpéné et al., 2018b; Carpéné et al., 2018c).

Additionally, phenelzine might mitigate obesity-associated alterations by acting on key molecular targets in oxidative stress, inflammation and glucose homeostasis. Excessive fat accumulation triggers oxidative stress that is responsible for the development of insulin resistance and cardiovascular disease (Bashan et al., 2009). Owing to its scavenging activity (Baker et al., 2019), phenelzine attenuates plasma protein carbonyl groups and lipid peroxidation induced by reactive species (Mustafa et al., 2017; Mustafa et al., 2018) and inhibits carbonyl stress accompanied by a reduction in atherosclerotic lesion (Galvani et al., 2008). Moreover, phenelzine reduces hepatic lipid peroxidation in high-sucrose drinking (HSD) mice (Carpéné et al., 2018b). Therefore, it would be interesting to explore whether phenelzine inhibits the increased oxidative stress associated with obesity and insulin resistance.

A chronic low-grade inflammation state is a characteristic of obesity in which the recruitment of immune cells in adipose tissue plays a pivotal role in the development of inflammation (Vachharajani and Granger, 2009). SSAO/VAP-1 participates in the rolling, adhesion and migration of leukocytes (Jalkanen and Salmi, 1993; Koskinen et al., 2004). SSAO/VAP-1 inhibitors reduce leukocyte extravasation and the expression of pro-inflammatory cytokines in experimental models of inflammation other than obesity (Koskinen et al., 2004; Salter-Cid et al., 2005; Wang et al., 2006; O'Rourke et al., 2008; Wang et al., 2018). Therefore, it is plausible that phenelzine inhibits low-grade inflammation in obese and insulin-resistant states.

The hypoglycaemic effect of phenelzine (McIntyre et al., 2006) may be caused by an inhibition of intestinal glucose uptake, hepatic gluconeogenesis, and alteration of pancreatic insulin release (Aleyassine and Gardiner, 1975; Feldman and Chapman, 1975; Haeckel and Oellerich, 1977; Haeckel et al., 1984). Given glycaemia restoration in HSD mice (Carpéné et al., 2018b), it becomes challenging to investigate whether phenelzine influences glucose homeostasis in insulin-resistant models.

To determine whether phenelzine affects obesity-associated metabolic disturbances, we analysed its effects on body fat accumulation, markers of oxidative stress and inflammation, and glucose and insulin homeostasis, in a model of diet-induced obesity and insulin resistance.

JPET Fast Forward. Published on July 3, 2019 as DOI: 10.1124/jpet.119.259895
This article has not been copyedited and formatted. The final version may differ from this version.

Methods

Animals, diet and treatment

All animal care and experimental procedures complied with the principles established by the Institut National de la Santé et de la Recherche Médicale (INSERM, France), under the permission number 12-1048-03-15 and were approved by the Animal Ethics Committee of the unit US006 CREFRE (Centre Régional d'Exploration Fonctionelle et Ressources Expérimentales, Toulouse, France).

Male C57BL/6 mice (Charles River, L'Arbresle, France) were housed for at least 2 weeks before treatment, in the INSERM US006 animal facility (three per cage) under 12/12 h light/dark cycle with controlled temperature (20-22ºC) and humidity (50-60%). Mice were 11 weeks old at the start of the experiment. All animal studies are in compliance with the ARRIVE guidelines (Kilkenny et al., 2010; McGrath and Lilley, 2015).

The study protocol was not subject to randomization, since mice were separated into two groups of 12 with equivalent mean body weight (28.2±1.0 and 28.1±0.5 g) five days before the start of the protocol. On day 0, standard chow (SAFE, Augy, France) was replaced by a high-fat diet containing 45% of the energy from fat (Research Diets, New Brunswick, NJ, USA). Mice received *ad libitum* either tap water for drinking (HFD), or phenelzine sulfate in the drinking water for 83 days (HFD+PHE) provided as a 0.028% solution (1.20 mM), as previously described (Carpéné et al., 2018b; Carpéné et al., 2018c). Body mass and food and water consumption were recorded twice a week.

In vivo determinations on awake animals

Non-fasting blood glucose was determined weekly between 15:00 and 16:00 with a glucose monitor (Roche Diagnostic, Mannheim, Germany), using a blood drop withdrawn from the tail. Fasting blood glucose and insulin levels were determined at week 10 of treatment, prior to an oral glucose tolerance test (OGTT), which was performed after an 8-h fasting. Mice given a 60% glucose solution (3 $g \cdot kg^{-1}$ body weight) via oral gavage and glucose levels were determined at time -30, 0, 15, 30, 45, 60 and 120 min. Fasting serum insulin levels were assessed by an ultrasensitive mouse insulin ELISA (Mercodia AB, Uppsala, Sweeden). Insulin resistance was calculated by the homeostatic model assessment of insulin resistance (HOMA-IR = glucose ($mmol \cdot L^{-1}$) x insulin ($\mu U \cdot L^{-1}$)/22.5), and two surrogate indexes of insulin sensitivity: quantitative insulin sensitivity

JPET Fast Forward. Published on July 3, 2019 as DOI: 10.1124/jpet.119.259895
This article has not been copyedited and formatted. The final version may differ from this version.

check index (QUICKI = 1/log glucose ($mg \cdot dL^{-1}$) + log insulin ($\mu U \cdot mL^{-1}$) + log non-esterified fatty acids (NEFA, $mmol \cdot L^{-1}$) and revised-QUICKI (R-QUICKI = 1/log glucose ($mg \cdot dL^{-1}$) + log insulin ($\mu U \cdot mL^{-1}$) + log NEFA ($mmol \cdot L^{-1}$), as previously described (Matthews et al., 1985; Katz et al., 2000; Perseghin et al., 2001). $\Delta I/\Delta G$ score was assessed as a glucose sensitivity index and calculated by measuring insulin and glucose concentrations 30 min before and 15 min after the oral glucose load.

Body composition was assessed at weeks 6, 8 and 11 of treatment by nuclear NMR with an EchoMRI 100™ 3-in-1 device (Echo Medical Systems, Houston, TX, USA).

Rectal temperature was measured within the first 4 h of the light cycle using a digital thermometer (Hanna Instruments, Woonsocket, RI, USA).

Indirect calorimetry was performed in 6 mice per group after 24 h of acclimatization in individual cages at week 8. O_2 consumption (VO_2) and CO_2 production (VCO_2) were measured (Oxylet; Panlab-Bioseb) in individual mice at 25-min intervals during a 24-h period. The respiratory quotient ($RQ = VCO_2/VO_2$) and energy expenditure (EE, in $kcal \cdot d^{-1} \cdot kg^{-1}$, $0.75 = 1.44 \times VO_2 \times [3.815 + 1.232 \times RQ]$) were calculated. Ambulatory activities of the mice were monitored by an infrared photocell beam interruption method (Sedacom; Panlab-Bioseb).

Tissue collection and composition analysis

Mice were sacrificed by cervical dislocation after overnight fasting. Troncular blood was collected in heparinised tubes and processed to obtain plasma samples. White adipose tissue (WAT) was dissected from subcutaneous inguinal (iWAT) and visceral epididymal (eWAT) and retroperitoneal plus perirenal (pWAT) anatomical locations, while brown adipose tissue (BAT) was dissected from the interscapular area (iBAT). Adiposomatic index was calculated as the percentage of the sum of dissected fat pads relative to body mass.

Fat pads, liver, heart and skeletal muscles from the hind leg were weighed, snap-frozen in liquid nitrogen and stored at -80°C until analysis. Portions of iWAT, eWAT, pWAT and liver, were also immediately processed to determine H_2O_2 release, lipogenesis and lipolysis. Tissue lipid content was assessed using the Dole method as in (DOLE and MEINERTZ, 1960). Tissue DNA content was fluorimetrically quantified using DNA from salmon testes (Sigma, Saint Louis, Missouri, USA). Tissue protein content was assessed with the BCA protein assay kit (Pierce, Rockford, IL, USA).

JPET Fast Forward. Published on July 3, 2019 as DOI: 10.1124/jpet.119.259895
This article has not been copyedited and formatted. The final version may differ from this version.

Spontaneous H_2O_2 release and amine oxidases activity

The spontaneous release of H_2O_2 by pieces of iWAT pad was immediately measured after sacrifice by using the fluorimetric Amplex Red method, as previously described (Carpéné et al., 2016). This method relies on the horseradish peroxidase-catalysed production of resorufin from 10-acetyl-3,7 dihydrophenoxazine and H_2O_2. Briefly, 30 mg of fresh intact iWAT pad pieces were incubated with the chromogenic mixture of 40 µM Amplex Red (Interchim, Montluçon, France) plus 4 U/mL horseradish peroxidase in phosphate buffer at pH 7.5. The H_2O_2 release was measured without any addition (spontaneous release), with 0.1 mM benzylamine (SSAO substrate), or with 0.1 mM benzylamine after 1 mM semicarbazide pre-incubation (to measure SSAO activity). After 30 min of incubation, samples were excited at 544 nm and fluorescence readouts at 590 nm were collected with the Fluoroskan Ascent microplate reader (ThermoLabsystems, Vantaa, Finland). To verify that the spontaneous release of H_2O_2 in iWAT was increased by HFD, we also measured it in 12 normal-weight male C57BL/6 mice of the same age (5 months old) fed a standard chow.

SSAO and MAO activities were similarly determined in thawed iWAT and liver homogenates with slight modifications (Zhou and Panchuk-Voloshina, 1997). Tissue homogenates were incubated in the presence of 0.5 mM tyramine or 0.1 mM benzylamine, with or without pre-incubation with 0.1 mM pargyline (to determine MAO component) or 1 mM semicarbazide (for SSAO component). H_2O_2 release was normalized to the protein content of the homogenate.

Lipogenesis and lipolysis

Adipocytes were isolated from eWAT and pWAT pads by digestion with 15 $\mu g \cdot ml^{-1}$ type TM liberase (Roche Diagnostics, Meylan, France) in Krebs-Ringer buffer supplemented with 15 mM bicarbonate, 10 mM HEPES, 2 mM pyruvate and 3.5% BSA, at 37ºC for 45 min. Once the tissue is digested, filtered and washed, lipogenesis was assessed as the radioactively labelled glucose incorporated into cellular lipids, as previously described (Harant-Farrugia et al., 2014). Briefly, adipocytes were incubated with a mixture of cold glucose and D-[3-^{3}H]-glucose (Perkin Elmer, Waltham, USA) for 120 min at 37ºC in the absence or presence of 0.1 µM insulin, 0.1 mM benzylamine, 0.1 mM vanadate, or 0.1 mM benzylamine plus 0.1 mM vanadate. Reactions were stopped by adding sulphuric acid and radioactivity was measured after adding a non-water-miscible liquid scintillation cocktail (InstaFluor-plus, Perkin Elmer). Cell lipid content

JPET Fast Forward. Published on July 3, 2019 as DOI: 10.1124/jpet.119.259895
This article has not been copyedited and formatted. The final version may differ from this version.

was extracted and quantified as described above.

Lipolytic activity was assessed by glycerol release as previously reported (Carpéné et al., 2007). Briefly, adipocytes were diluted 10x in KRBH buffer. Samples at a final volume of 0.4 mL were incubated for 90 min in the absence or presence of 1 µM isoprenaline or 1 µM isoprenaline plus 1 mM tyramine. Glycerol released was referred to 100 mg of cellular lipids.

Gene expression

Total RNA was isolated from iWAT, pWAT, iBAT, liver and skeletal muscle, following the chloroform/isopropanol method using Qiazol (Qiagen, Hilden, Germany) to homogenize tissues. RNA was reverse transcribed using Superscript II reverse transcriptase (Life Technologies Corporation, Carlsbad, USA) and random hexamers. Real-time PCR was performed in a Step One Plus system (Applied Biosystems, Warrington, USA), using the SYBR Green Master Mix (Eurogentec, Liège, Belgium). Oligonucleotide primers were designed and are available upon request. Relative gene expression was calculated using the $2^{-\Delta\Delta Ct}$ method with 18S ribosomal RNA as internal control.

Oxidative stress-related parameters

Aconitase activity was measured with a spectrophotometric assay (OxisResearch, Foster City, CA, USA). Lipid peroxidation was determined by measuring the formation of malondialdehyde, with a TBARS assay kit (Cayman Chemical Company, Ann Arbor, MI, USA).

Other circulating parameters

Fasting NEFAs, triacylglycerols, LDL-cholesterol, HDL-cholesterol, phosphatase alkaline, alanine aminotransferase and urea plasma levels were determined by using an autoanalyzer (Cobas Roche Diagnostic, Basel, Switzerland). Fasting circulating glycerol was determined by using an enzymatic colorimetric kit (Sigma-Aldrich, Saint-Quentin-Fallavier, France).

Data and statistical analysis

The data and statistical analysis comply with the recommendations on experimental design and analysis in pharmacology (Curtis et al., 2018). Normal

JPET Fast Forward. Published on July 3, 2019 as DOI: 10.1124/jpet.119.259895
This article has not been copyedited and formatted. The final version may differ from this version.

distribution of the data was tested using the Shapiro-Wilk test. Log-transformation was applied before the analysis if variables were not adjusted to parametric criteria. Data are given as mean ± SEM of the indicated number of independent observations and were analysed comparing two experimental groups by Student's t-test or Mann-Whitney U test for parametric and non-parametric distributions, respectively. Two-way repeated measures ANOVA followed by a Bonferroni post-hoc test were used for multiple measures analysis. Statistical significance was assumed when $P<0.05$. Calculations were made with IBM SPSS Statistics, version 25.0 (IBM Corp, Armonk, NY, USA) and were represented with GraphPad Prism version 8.0.0.

Materials

Phenelzine sulphate (P6777 from Sigma-Aldrich-Merck) was dissolved weekly in tap water to provide enough drinking solution to the treated mice. Most of the other reagents were from Sigma-Aldrich-Merck, unless otherwise stated. Isoprenaline, identical to (-)-isoproterenol, was a generous gift from A. Mairal (I2MC, Toulouse, France).

Results

1. Oral chronic phenelzine treatment reduces body adiposity in HFD mice

HFD+PHE mice showed a lower body weight than HFD mice as early as the first week of treatment (Figure 1A). This difference was maintained throughout most of the treatment, and by the end of it, HFD+PHE mice weighed 11% less vs. HFD. These differences could not be explained by decreased food consumption (Figure 1B), or lean tissue hydration (data not shown). Consequently, energy efficiency was lower in HFD+PHE (Figure 1 C).

However, body weight reduction could be attributable to reduced body fat content, which was 29%, 27% and 20% lower at weeks 6, 8 and 11, respectively (Figure 1D). Phenelzine treatment differentially affected the weight and lipid content of the distinct fat pads, particularly in subcutaneous pads. The weights of iWAT and iBAT were lower, whereas those of eWAT and pWAT were unchanged (Table 1). The adiposomatic index was not significantly reduced in HFD+PHE mice ($p=0.157$). Tissue composition analysis revealed that, in line with pad weights, total lipid content was reduced in iWAT and iBAT of HFD+PHE mice. In addition, DNA content in both iWAT and eWAT, as well as

protein content in the eWAT, were lower in HFD+PHE mice, suggesting that the number of cells could be reduced by phenelzine in iWAT and, despite the lack of differences in total lipid content and pad weight, also in eWAT (Table 1). Interestingly, the anti-fattening effect of phenelzine treatment was evidenced ectopically, in accordance with previous observations (Carpéné et al., 2018b; Carpéné et al., 2018c). Thus, lipid content in liver and skeletal muscle was, respectively, 58% and 34% lower in HFD+PHE animals (Table 1).

Importantly, phenelzine treatment normalized the circulating levels of alanine aminotransferase (HFD: 76.5±13.2 $U \cdot L^{-1}$, HFD+PHE: 32.7±4.7 $U \cdot L^{-1}$, $P<0.01$) and alkaline phosphatase (HFD: 24.8±3.3 $U \cdot L^{-1}$, HFD+PHE: 14.8±2.5 $U \cdot L^{-1}$, $P<0.05$). Lack of increase in transaminases concentration, together with unaltered circulating urea levels (HFD: 7.6±0.3 mM, HFD+PHE: 7.9±0.5 mM, $P=0.591$), indicated that this treatment was not hepato- or nephro-toxic.

2. *Adipose and hepatic SSAO and MAO activities are inhibited by phenelzine treatment*

The calculated daily phenelzine intake was 20.8±1.6 mg (88.9±6.7 µmols) per kg of body weight. It was estimated from previous experiments in normal-weight mice that chronic exposure to a 1.2 mM phenelzine drinking solution could inhibit adipose SSAO and MAO activities in mice fed a HFD (Carpéné et al., 2018c). AO activities were measured to confirm they were inhibited. As expected, benzylamine, and to a lesser extent, tyramine, were preferentially oxidized by SSAO rather than MAO in iWAT homogenates (Figures 2A-B). Collectively, total benzylamine oxidation was inhibited by 83% in iWAT homogenates of HFD+PHE mice (Figure 2A). Phenelzine treatment almost completely blocked benzylamine oxidation by SSAO activity (by 82%) and reduced MAO activity to negligible levels. Similarly, phenelzine treatment inhibited the tyramine oxidation by SSAO (80%), MAO (89%) and both AO (79%) activities (Figure 2B).

In liver homogenates, tyramine and benzylamine were more oxidized by MAO than by SSAO (Figure 2C-D). Phenelzine treatment inhibited benzylamine oxidation by MAO (86%) and SSAO (61%) activities, and total benzylamine oxidation was reduced by 66% (Figure 2C). Likewise, treatment inhibited tyramine oxidation by MAO (96%), SSAO (82%) and both (84%) activities (Figure 2D).

To further explore the mechanism of SSAO and MAO regulation by phenelzine, we analysed whether it regulates AOs at the transcriptional level. Hence, we determined

JPET Fast Forward. Published on July 3, 2019 as DOI: 10.1124/jpet.119.259895
This article has not been copyedited and formatted. The final version may differ from this version.

the mRNA expression of Aoc3, the gene that encodes SSAO, and MAO isoforms, MAO-A and MAO-B, in iWAT and liver. *Aoc3*, *Maoa* and *Maob* mRNA levels were all reduced in iWAT, indicating that phenelzine regulates SSAO and MAO at the transcriptional level in adipose tissue (Figure 2E). Similarly, in liver, *Maoa* and *Maob* mRNA levels were reduced, whilst *Aoc3* mRNA levels were increased, suggesting opposing mechanisms for SSAO regulation in the liver (Figure 2F).

3. *Phenelzine inhibits lipid metabolism genes, and reduces amine-induced lipogenesis and anti-lipolysis in adipocytes*

We investigated the potential effect of phenelzine treatment on the expression of key genes in lipid biosynthesis in HFD mice, particularly of those shown to be regulated by phenelzine (Chiche et al., 2009; Carpéné et al., 2018b; Carpéné et al., 2018c), in pWAT, iWAT, iBAT and liver (Figure 3A). PPARγ2 is the master regulator of adipocyte differentiation that transcriptionally controls the genes involved in lipid biosynthesis and uptake. In HFD+PHE mice, *Pparg2* mRNA levels were reduced in pWAT and iWAT by 34% and 66%, respectively. SREBP1c is a transcription factor that controls the expression of lipogenic genes, such as fatty acid synthase (*Fas*). *Srebp1c* mRNA levels were lower in iWAT (61%), iBAT (29%) and liver (49%), whilst *Fas* mRNA levels were reduced in iWAT (75%) and liver (71%) of HFD+PHE mice. Lastly, PEPCK is a key enzyme in adipose fatty acid reesterification, and mRNA levels were reduced in iWAT (39%), and in liver (30%).

De novo lipogenesis has been shown to be impaired in isolated adipocytes acutely treated with phenelzine (Carpéné et al., 2013) and in adipocytes from mice chronically exposed an oral solution of phenelzine (Carpéné et al., 2018c). Phenelzine treatment did not affect basal or 100 nM insulin-stimulated glucose incorporation into lipids, and did not alter the modest responses to 100 µM benzylamine or 100 µM vanadate (Figure 3B). However, in the presence of 100 µM benzylamine plus 100 µM vanadate, only the HFD group exhibited a stimulation of glucose incorporation into lipids.

To investigate whether lipid mobilisation was involved in the adiposity reduction observed, we first analysed the expression of the hormone-sensitive lipase (HSL), one of the major components of the lipolytic cascade, and found that mRNA levels were lower in the iWAT of phenelzine-drinking mice (Figure 3A). Then, we assessed the potential effect of chronic phenelzine treatment on the lipolytic action of isoprenaline in visceral adipocytes. Neither basal nor 1 µM isoprenaline-stimulated glycerol release were affected

JPET Fast Forward. Published on July 3, 2019 as DOI: 10.1124/jpet.119.259895
This article has not been copyedited and formatted. The final version may differ from this version.

by phenelzine (Figure 3C). Furthermore, we assessed the anti-lipolytic action of tyramine on isoprenaline-induced lipolysis. As expected, the anti-lipolytic action of 1 mM tyramine was observed in HFD mice in which isoprenaline-induced lipolysis was reduced by 26%. On the contrary, the anti-lipolytic effect of tyramine was not evidenced in HFD+PHE mice. Based on our previous observations of the AO-dependency of the anti-lipolytic effect of tyramine (Carpéné et al., 2018a), it is likely that the inhibition of adipose AO activity in HFD+PHE induces the disappearance of such tyramine effect in their adipocytes.

4. Phenelzine reduces H_2O_2 production in fresh iWAT

First, we verified that the spontaneous release of H_2O_2 by freshly isolated iWAT was increased by HFD. H_2O_2 release in HFD mice was 3-fold higher than in standard chow-fed mice (HFD vs. CON: 0.127±0.018 vs. 0.040±0.009 nmols H_2O_2/min/mg protein; $P<0.001$), confirming that HFD increases oxidative stress in adipose tissue (Sonta et al., 2004). Remarkably, the spontaneous release of H_2O_2 relative to protein content or tissue weight was reduced in HFD+PHE mice by 59% and 37%, respectively (Figure 4A). In response to 100 µM benzylamine, H_2O_2 levels tended to increase in HFD mice, whereas they remained low in HFD+PHE mice, suggesting that the AO-produced H_2O_2 was blocked. The pre-incubation of 1 mM semicarbazide with iWAT allowed us to estimate SSAO activity and, in accordance with the assays performed in iWAT homogenates, we confirmed that SSAO activity was almost abolished by phenelzine treatment (HFD vs. HFD+PHE: 0.208±0.057 vs. 0.055±0.018 nmols H_2O_2/min/mg protein; $P<0.05$).

Markers of oxidative stress in other organs were not modified by treatment, including hepatic and plasma malondialdehyde levels (Figure 4B) and hepatic and cardiac aconitase activity (Figure 4C).

5. Phenelzine reduces the expression of inflammatory-related genes in WAT and liver

We hypothesized that phenelzine treatment inhibits low-grade inflammation in HFD mice, since it potently inhibits SSAO/VAP-1 activity (Carpéné et al., 2008) and SSAO/VAP-1 deficiency reduces leukocyte infiltration in adipose tissue (Bour et al., 2009). To investigate it, we analysed the expression of genes involved in immune cell infiltration, namely monocyte chemoattractant protein 1 (*Mcp1*), *Cd45* and *F4/80*, and

JPET Fast Forward. Published on July 3, 2019 as DOI: 10.1124/jpet.119.259895
This article has not been copyedited and formatted. The final version may differ from this version.

pro-inflammatory cytokines, namely IL-6, IL-10 and TNF-α, in adipose tissue and liver (Figure 5). In the pWAT, phenelzine reduced the mRNA levels of *Mcp1* by 50%, *Cd45* by 54%, *Il6* by 57% and *Tnf* by 43%, whilst *F4/80* and *Il10* mRNA levels showed a tendency to decrease. In the iWAT, *Cd45* mRNA levels were also reduced in HFD+PHE mice by 57%, and *Tnf* mRNA levels showed a tendency to decrease. In the liver, phenelzine administration also reduced the mRNA levels of the pro-inflammatory cytokines *Tnf* (58%) and *Il6* (75%).

6. Phenelzine treatment improves circulating lipid profile

We analysed whether body adiposity mitigation in HFD+PHE mice could be accompanied by changes in the circulating lipid profile. Plasma NEFAs levels were elevated in HFD mice, but phenelzine treatment did not modify them (Figure 6A). Plasma glycerol and triacylglycerol levels were both reduced in HFD+PHE mice by 30% and 16%, respectively. Regarding circulating cholesterol levels, there were no differences in LDL-cholesterol, whilst HDL-cholesterol levels were a 12% lower in HFD+PHE. The unexpected reduction in the circulating levels of HDL-cholesterol prompted us to investigate whether phenelzine treatment triggered any alteration in the expression of a key gene in HDL-cholesterol uptake into cells, scavenger receptor class B type 1 (*Sr-b1*). Consistent with decreased HDL-cholesterol levels, mRNA levels of *Srb1* in the liver were 38% lower in HFD+PHE mice (Figure 6B).

7. Phenelzine reduces insulinemia without affecting glycaemia

No reduction in non-fasting glycaemia was observed in the weekly determinations during treatment in HFD+PHE mice (data not shown). Fasting glycaemia was not changed by treatment, whilst insulinemia was markedly reduced by 55% (Figure 7A). HOMA-IR score indicated that HFD mice developed insulin resistance, whereas in HFD+PHE animals it was found to be 59% lower, suggesting less insulin resistance (Figure 7B). This was also supported by QUICKI and R-QUICKI indexes, both 10% higher in HFD+PHE mice. ΔI/ΔG score was lower in HFD+PHE mice, suggesting an increased insulin response to glucose (Figure 7B). However, there were no differences in glucose tolerance after the oral glucose load (Figure 7C).

8. Phenelzine triggers signs of higher EE, despite no major impact on oxidative metabolism capacity

JPET Fast Forward. Published on July 3, 2019 as DOI: 10.1124/jpet.119.259895
This article has not been copyedited and formatted. The final version may differ from this version.

An increased half-life of catecholamine and trace amine levels can be expected after a chronic MAO inhibition which, in turn, could impact oxidative metabolism and thus be involved in the mitigation of the HFD-induced metabolic disturbances. To investigate whether phenelzine treatment influences oxidative metabolism in HFD mice, we assessed rectal temperature, EE and locomotor activity.

Rectal temperature was higher in HFD+PHE vs. HFD mice (Figure 8A). VO_2, VCO_2, RQ and EE were also higher in HFD+PHE mice at certain time-points according student's *t*-test, particularly during the first part of the night period. However, there were no significant differences in any of these parameters after two-way repeated measures ANOVA or when considering the mean values of these data collected within the diurnal, night or 24 h periods (Figure 8B-E), only a tendency to higher VCO_2 and EE. Furthermore, there were no differences regarding the circadian activity (Figure 8F) and the number of rears (not shown).

To gain insight into the potential phenelzine effect on EE, the expression of genes involved in fuel utilization and thermogenesis was analysed in iBAT, liver and skeletal muscle (Table 2). In the iBAT, carnitine palmitoyltransferase 1B (*Cpt1b*) mRNA levels were increased by 22% in HFD+PHE mice. *Vegf* expression, which is up-regulated under BAT activation, tended to increase in HFD+PHE mice. However, *Ppar* alpha (*Ppara*), *Ppar* coactivator gamma 1α (*Ppargc1a*), forkhead box C2 (*Foxc2*) and uncoupling protein 1 (*Ucp1*) mRNA levels were unchanged. Hepatic acetyl carboxylase 2 (*Acc2*) and *Ppara* mRNA levels were reduced (47% and 52%, respectively), suggesting opposing effects on lipid catabolism. In skeletal muscle, cluster of differentiation 36 (*Cd36*) and uncoupling protein 3 (*Ucp3*) mRNA levels were not affected by treatment, whilst those of *Ppargc1a* and glucose transporter 4 (*Glut4*) tended to decrease, and those of *Ppara* and *Cpt1b* were even reduced, by 31% and 25%, respectively.

Discussion

In this study, we demonstrated that oral chronic phenelzine treatment reduces metabolic alterations developed by a HFD in mice, including subcutaneous and hepatic fat, hypertriglyceridemia, insulin resistance, and markers of oxidative stress, leukocyte infiltration and inflammation. Moreover, this animal model has allowed us to further determine factors and molecular mechanisms involved in the metabolic effects of phenelzine, particularly on fat accumulation, comparing with the effects on other animal models (Carpéné et al., 2008; Carpéné et al., 2018b). Thus, reduced adiposity by different

phenelzine treatments has been demonstrated in female obese Zucker rats, male mice on a HSD, showing differing results regarding the adipose tissues affected and the mechanisms involved. Only subcutaneous fat pads were decreased in mice on a HFD (present study) or HSD (Carpéné et al., 2018b), whilst visceral fat pads were the only ones decreased in obese Zucker rats (Carpéné et al., 2008). This suggests that several factors, including diet, species, sex or drug administration route, could explain the depot-specific impact of phenelzine on fat stores. According to our results, the limitation of adiposity could be partly attributed to a blockade of SSAO activity associated with an inhibition of amine-induced *de novo* lipogenesis (Carpéné et al., 2008). The involvement of SSAO inhibition on reducing fat accumulation has been previously demonstrated by the use of other SSAO inhibitors, including semicarbazide (Carpéné et al., 2008; Mercader et al., 2011) and aminoguanidine (Prévot et al., 2007), both showing a lower potency on SSAO inhibition than phenelzine (Carpéné et al., 2008). On the contrary, our data do not support a major role in lipid mobilisation since: 1) plasma NEFA and glycerol did not increase, 2) visceral WAT depot weights were unaffected, and 3) *Hsl* was down-regulated in iWAT.

SSAO-independent mechanisms could also be involved in the phenelzine-induced reduction of fat accumulation. Indeed, phenelzine impairs not only the amine-induced, but also the insulin-stimulated *de novo* lipogenesis in isolated adipocytes (Carpéné et al., 2013; Carpéné et al., 2014) and in normal-weight mice after chronic treatment (Carpéné et al., 2018c). In the present study, however, the lipogenic action of insulin was not impaired, as was the case for phenelzine-treated obese Zucker rats and HSD mice (Carpéné et al., 2008; Carpéné et al., 2018b). This observation suggests that the ability of phenelzine to inhibit the lipogenic action of insulin could be surpassed in obesity and insulin resistance models. Another target that could mediate the long-term inhibitory effect of phenelzine on lipogenesis and adipocyte differentiation is SREBP-1c, as shown in cultured differentiating adipocytes (Chiche et al., 2009). In HFD+PHE mice, the expression of *Srebp1c* and its controlled gene *Fas* were lower in iWAT and liver and were unchanged in pWAT, where lipid content was unaffected. Furthermore, *Srebp1c* expression was unchanged in normal-weight and HSD mice after phenelzine treatments (Carpéné et al., 2018b; Carpéné et al., 2018c), despite fat pad reduction, suggesting that the drug effect on *Srebp1c* is diet-dependent. Unlike HFD, fructose supplementation strongly induces *Srebp1c* mRNA expression (Softic et al., 2017). Thus, the inhibitory phenelzine effect on *Srebp1c* mRNA could occur particularly under a low carbohydrate

intake, as in HFD, and be masked by the high fructose intake of mice on a HSD, as well as in standard chow-fed mice having high-carbohydrate intake. Additionally, inhibition of fatty acid re-esterification could be involved in the reduced fat accumulation in liver and iWAT since both hepatocytes and adipocytes synthesize triacylglycerols using PEPCK-produced glycerol-3-phosphate (Prentki and Madiraju, 2008). This is suggested by the lower circulating glycerol and hepatic and adipose *Pepck* expression in HFD+PHE mice. Moreover, epigenetic mechanisms might be involved in the depot-specific phenelzine effects on adipose cells since the drug affects the differentiation of stem cells by modulating histone methylation status (Yan et al., 2016).

Our results suggest a reduction of hepatic steatosis and inflammation, which could contribute to the amelioration of liver function, as shown by the normalization of transaminase levels. The lower hepatic lipid content together with the reduced triglyceridemia in HFD+PHE mice suggest that the hepatic triacylglycerol synthesis capacity could be impaired, which is supported by the reduced *Srebp1c*, *Fas* and *Pepck* expression. Furthermore, the reduction of the HFD-induced pro-inflammatory state is supported by the reduced expression of IL-6 and TNF-α cytokines, which were also inhibited by phenelzine in other models of inflammation (Ekuni et al., 2009; Li et al., 2018). Remarkably, the phenelzine effect on these cytokines also occurs in the adipose tissue, more conspicuously in the visceral pad in which the inflammatory status is higher than in the subcutaneous pad. In addition, the inhibition of the enzymatic SSAO/VAP-1 activity, observed in both liver and adipose tissue of HFD+PHE mice, could mediate the reduced hepatic and adipose inflammation, since the catalytic activity is required in its role in leukocyte transmigration and inflammation (Koskinen et al., 2004; Weston et al., 2015). The combined down-regulation of pro-inflammatory cytokines and of leukocyte infiltration markers, seen in liver, pWAT and iWAT, supports the inhibitory role of the hydrazine on the low-grade inflammation associated with obesity.

Interestingly, the reduction of fat accumulation and body weight was not accompanied by changes in food consumption, in accordance with the previous results obtained in mice with different dietary conditions (Carpéné et al., 2018b; Carpéné et al., 2018c) or phenelzine-injected rats (Carpéné et al., 2008). This observation contrasts with the higher food intake and craving reported in phenelzine-treated patients and with the inhibitory effect on food consumption induced by semicarbazide that contributes to reduced body weight (Carpéné et al., 2007; Carpéné et al., 2008; Mercader et al., 2011) and seems to indicate that neuronal transmission is exquisitely regulated by

monaminergic systems that are differentially regulated upon MAO inhibition.

The hypoglycaemic effect of phenelzine reported in patients with depression and mood disorders (McIntyre et al., 2006) has been explained by hepatic gluconeogenesis inhibition, intestinal glucose uptake impairment and/or enhanced insulin release (Aleyassine and Gardiner, 1975; Feldman and Chapman, 1975; Haeckel and Oellerich, 1977; Haeckel et al., 1984). According to an *in vitro* study with high phenelzine doses, the effect on insulin release is, however, the opposite (Aleyassine and Gardiner, 1975). Therefore, it is relevant to investigate whether phenelzine can reduce hyperglycaemia and hyperinsulinemia in animal models of obesity and insulin resistance. Interestingly, in HSD mice, which did not develop insulin resistance, phenelzine restored high glucose levels (Carpéné et al., 2018b). However, considering that the insulin-like effect of AO substrates on glucose transport in adipocytes depends on their oxidation (Visentin et al., 2005; Mercader et al., 2010), it remains difficult to understand how AO inhibitors can reduce hyperglycaemia or improve glucose tolerance. Here, in insulin-resistant mice, phenelzine did not affect hyperglycaemia and glucose tolerance. However, HFD+PHE mice consistently attenuated hyperinsulinemia and insulin resistance. Since both fasting and feeding glycaemia were not changed by phenelzine treatment, it is unlikely that a strong inhibition of hepatic gluconeogenesis and intestinal glucose uptake occurred in HFD+PHE mice. A direct effect on insulin release through a MAO-independent mechanism cannot be excluded (Feldman and Chapman, 1975), despite the dose at which phenelzine could inhibit insulin release (Aleyassine and Gardiner, 1975) is not expected to be reached in HFD+PHE mice. In addition, the amelioration of insulin sensitivity could be an indirect consequence of the treatment as a result of the reduced adiposity, pro-inflammatory cytokine and/or H_2O_2 production.

The lack of reduction of malondialdehyde is apparently disappointing since phenelzine is endowed with scavenging properties towards aldehydes and oxidative stress (Galvani et al., 2008; Baker et al., 2019). Two hypotheses can explain this: 1) the protective effect of phenelzine was probably insufficient to limit the dramatic increase of systemic markers of oxidative stress developed by HFD (Sonta et al., 2004), and 2) the changes in malondialdehyde plasma levels did not reflect the complex and depot-specific changes in lipid peroxidation products occurring in adipose tissue (Long et al., 2013).

Rectal temperature, an indicator of EE, was increased by phenelzine, as in HSD mice (Carpéné et al., 2018b). Such thermogenic effect of phenelzine might be caused by increased 5-HT levels, which together with noradrenaline controls body temperature

(Bruinvels and Kemper, 1971). The potential phenelzine-induced BAT activation seems to not occur in HFD mice, but it cannot be ruled out since an increased *Cpt1* mRNA expression suggests a higher fatty acid beta-oxidation rate. Regardless of the lack of dramatic BAT recruitment, we further evaluated the potential changes in EE, which could have been produced by the elevation in catecholamine and trace amine levels after AO inhibition (Baker et al., 2000). Accordingly, a local increase in catecholamine levels induced by the administration of reuptake inhibitors caused weight loss by increasing locomotor activity and thermogenesis (Billes and Cowley, 2008). Phenelzine could increase EE by enhancing the spontaneous locomotor activity since it decreases immobility time in the forced-swim test (Zhao et al., 2009) and attenuates motor-suppressant effects (McManus and Greenshaw, 1991). The increased activity is thought to be mediated by reducing either α- and β_2-adrenoreceptor sensitivity (McManus and Greenshaw, 1991; McKenna et al., 1992; Paetsch and Greenshaw, 1993). The latter is attributed to an increase in 2-phenylethylamine (McManus and Greenshaw, 1991), a phenelzine metabolite (Baker et al., 2000), which reduces, as phenelzine, the behavioural response to a β_2-adrenoceptor agonist (Paetsch and Greenshaw, 1993) and is associated with a decrease in body weight (Pawar and Grundel, 2017). However, lack of changes in the locomotor activity suggests that it does not contribute to the attenuation of metabolic disturbances exhibited by phenelzine-drinking mice, further supported by the lack of increase in the expression of genes involved in fuel utilisation in the skeletal muscle. Oxygen consumption, RQ and EE tended to be higher in HFD+PHE mice. Unfortunately, these parameters were in six animals per group only, therefore reducing statistical power.

The exciting findings reported in this study indicate that phenelzine mitigates several metabolic alterations developed by a HFD. Further studies are warranted to perhaps consider phenelzine as useful for a multi-therapy treatment of obesity and its cardiovascular and neurologic complications.

Acknowledgements: J Mercader was funded by the European grant INTERREG IVB SUDOE 1/P1/E178 “DIOmed Project”. The authors are grateful to Estelle Wanecq (I2MC, Toulouse) for help in RNA extraction and to Antonio Zorzano (IRB, Barcelona) for facilitating collaborations beyond DIOmed project.

Authorship Contributions

Participated in research design: Mercader and Carpéné

Conducted experiments: Mercader, Le Gonidec, Decaunes, Gómez-Zorita, and Carpéné

Performed data analysis: Mercader, Sabater, Le Gonidec, and Carpéné

Wrote or contribute to the writing of the manuscript: Mercader, Chaplin, Milagro, Carpéné.

References

Aleyassine H and Gardiner RJ (1975) Dual action of antidepressant drugs (MAO inhibitors) on insulin release. *Endocrinology* **96**:702-710.

Baker G, Matveychuk D, MacKenzie EM, Holt A, Wang Y and Kar S (2019) Attenuation of the effects of oxidative stress by the MAO-inhibiting antidepressant and carbonyl scavenger phenelzine. *Chem Biol Interact*.

Baker GB, Coutts RT and Greenshaw AJ (2000) Neurochemical and metabolic aspects of antidepressants: an overview. *J Psychiatry Neurosci* **25**:481-496.

Bashan N, Kovsan J, Kachko I, Ovadia H and Rudich A (2009) Positive and negative regulation of insulin signaling by reactive oxygen and nitrogen species. *Physiol Rev* **89**:27-71.

Billes SK and Cowley MA (2008) Catecholamine reuptake inhibition causes weight loss by increasing locomotor activity and thermogenesis. *Neuropsychopharmacology* **33**:1287-1297.

Bour S, Caspar-Bauguil S, Iffiú-Soltész Z, Nibbelink M, Cousin B, Miiluniemi M, Salmi M, Stolen C, Jalkanen S, Casteilla L, Pénicaud L, Valet P and Carpéné C (2009) Semicarbazide-sensitive amine oxidase/vascular adhesion protein-1 deficiency reduces leukocyte infiltration into adipose tissue and favors fat deposition. *Am J Pathol* **174**:1075-1083.

Bruinvels J and Kemper GC (1971) Role of noradrenaline and 5-hydroxytryptamine in tetrahydronaphthylamine-induced temperature changes in the rat. *Br J Pharmacol* **43**:1-9.

Carpéné C, Abello V, Iffiú-Soltész Z, Mercier N, Fève B and Valet P (2008) Limitation of adipose tissue enlargement in rats chronically treated with semicarbazide-sensitive amine oxidase and monoamine oxidase inhibitors. *Pharmacol Res* **57**:426-434.

Carpéné C, Boulet N, Chaplin A and Mercader J (2019) Past, Present and Future Anti-Obesity Effects of Flavin-Containing and/or Copper-Containing Amine Oxidase Inhibitors. *Medicines (Basel)* **6**.

Carpéné C, Galitzky J, Belles C and Zakaroff-Girard A (2018a) Mechanisms of the antilipolytic response of human adipocytes to tyramine, a trace amine present in food. *J Physiol Biochem* **74**:623-633.

Carpéné C, Gomez-Zorita S, Gupta R, Grès S, Rancoule C, Cadoudal T, Mercader J, Gomez A, Bertrand C and Iffiu-Soltész Z (2014) Combination of low dose of the anti-adipogenic agents resveratrol and phenelzine in drinking water is not sufficient to prevent obesity in very-high-fat diet-fed mice. *Eur J Nutr* **53**:1625-1635.

Carpéné C, Grès S and Rascalou S (2013) The amine oxidase inhibitor phenelzine limits lipogenesis in adipocytes without inhibiting insulin action on glucose uptake. *J Neural Transm (Vienna)* **120**:997-1003.

Carpéné C, Gómez-Zorita S, Chaplin A and Mercader J (2018b) Metabolic Effects of Oral Phenelzine Treatment on High-Sucrose-Drinking Mice. *Int J Mol Sci* **19**.

Carpéné C, Iffiú-Soltesz Z, Bour S, Prévot D and Valet P (2007) Reduction of fat deposition by combined inhibition of monoamine oxidases and semicarbazide-sensitive amine oxidases in obese Zucker rats. *Pharmacol Res* **56**:522-530.

Carpéné C, Les F, Hasnaoui M, Biron S, Marceau P, Richard D, Galitzky J, Joanisse DR and Mauriège P (2016) Anatomical distribution of primary amine oxidase activity in four adipose depots and plasma of severely obese women with or without a dysmetabolic profile. *J Physiol Biochem* **73**:475-486.

Carpéné C, Mercader J, Le Gonidec S, Schaak S, Mialet-Perez J, Zakaroff-Girard A and Galitzky J (2018c) Body fat reduction without cardiovascular changes in mice after oral treatment with the MAO inhibitor phenelzine. *Br J Pharmacol* **175**:2428-2440.

Chiche F, Le Guillou M, Chétrite G, Lasnier F, Dugail I, Carpéné C, Moldes M and Fève B (2009) Antidepressant phenelzine alters differentiation of cultured human and mouse preadipocytes. *Mol Pharmacol* **75**:1052-1061.

Curtis MJ, Alexander S, Cirino G, Docherty JR, George CH, Giembycz MA, Hoyer D, Insel PA, Izzo AA, Ji Y, MacEwan DJ, Sobey CG, Stanford SC, Teixeira MM, Wonnacott S and Ahluwalia A (2018) Experimental design and analysis and their reporting II: updated and simplified guidance for authors and peer reviewers. *Br J Pharmacol* **175**:987-993.

DOLE VP and MEINERTZ H (1960) Microdetermination of long-chain fatty acids in plasma and tissues. *J Biol Chem* **235**:2595-2599.

Ekuni D, Firth JD, Nayer T, Tomofuji T, Sanbe T, Irie K, Yamamoto T, Oka T, Liu Z, Vielkind J and Putnins EE (2009) Lipopolysaccharide-induced epithelial monoamine oxidase mediates alveolar bone loss in a rat chronic wound model. *Am J Pathol* **175**:1398-1409.

Feldman JM and Chapman B (1975) Monoamine oxidase inhibitors: nature of their interaction with rabbit pancreatic islets to alter insluin secretion. *Diabetologia* **11**:487-494.

Galvani S, Coatrieux C, Elbaz M, Grazide MH, Thiers JC, Parini A, Uchida K, Kamar N, Rostaing L, Baltas M, Salvayre R and Nègre-Salvayre A (2008) Carbonyl scavenger and antiatherogenic effects of hydrazine derivatives. *Free Radic Biol Med* **45**:1457-1467.

Haeckel R and Oellerich M (1977) The influence of hydrazine, phenelzine and nialamide on gluconeogenesis and cell respiration in the perfused guinea-pig liver. *Eur J Clin Invest* **7**:393-400.

Haeckel R, Terlutter H, Schumann G and Oellerich M (1984) Hydrazonopropionic acids, a new class of hypoglycemic substances, 3. Inhibition of jejunal glucose uptake in the rat and guinea pig. *Horm Metab Res* **16**:423-427.

Harant-Farrugia I, Garcia J, Iglesias-Osma MC, Garcia-Barrado MJ and Carpéné C (2014) Is there an optimal dose for dietary linoleic acid? Lessons from essential fatty acid deficiency supplementation and adipocyte functions in rats. *J Physiol Biochem* **70**:615-627.

Iglesias-Osma MC, Garcia-Barrado MJ, Visentin V, Pastor-Mansilla MF, Bour S, Prévot D, Valet P, Moratinos J and Carpéné C (2004) Benzylamine exhibits insulin-like effects on glucose disposal, glucose transport, and fat cell lipolysis in rabbits and diabetic mice. *J Pharmacol Exp Ther* **309**:1020-1028.

Jalkanen S and Salmi M (1993) A novel endothelial cell molecule mediating lymphocyte binding in humans. *Behring Inst Mitt*:36-43.

Katz A, Nambi SS, Mather K, Baron AD, Follmann DA, Sullivan G and Quon MJ (2000) Quantitative insulin sensitivity check index: a simple, accurate method for assessing insulin sensitivity in humans. *J Clin Endocrinol Metab* **85**:2402-2410.

Kilkenny C, Browne W, Cuthill IC, Emerson M, Altman DG and Group NRRGW (2010) Animal research: reporting in vivo experiments: the ARRIVE guidelines. *Br J Pharmacol* **160**:1577-1579.

Koskinen K, Vainio PJ, Smith DJ, Pihlavisto M, Ylä-Herttuala S, Jalkanen S and Salmi M (2004) Granulocyte transmigration through the endothelium is regulated by the oxidase activity of vascular adhesion protein-1 (VAP-1). *Blood* **103**:3388-3395.

Li R, Sahu S and Schachner M (2018) Phenelzine, a small organic compound mimicking the functions of cell adhesion molecule L1, promotes functional recovery after mouse spinal cord injury. *Restor Neurol Neurosci* **36**:469-483.

Long EK, Olson DM and Bernlohr DA (2013) High-fat diet induces changes in adipose tissue trans-4-oxo-2-nonenal and trans-4-hydroxy-2-nonenal levels in a depot-specific manner. *Free Radic Biol Med* **63**:390-398.

Matthews DR, Hosker JP, Rudenski AS, Naylor BA, Treacher DF and Turner RC (1985) Homeostasis model assessment: insulin resistance and beta-cell function from fasting plasma glucose and insulin concentrations in man. *Diabetologia* **28**:412-419.

McGrath JC and Lilley E (2015) Implementing guidelines on reporting research using animals (ARRIVE etc.): new requirements for publication in BJP. *Br J Pharmacol* **172**:3189-3193.

McIntyre RS, Soczynska JK, Konarski JZ and Kennedy SH (2006) The effect of antidepressants on glucose homeostasis and insulin sensitivity: synthesis and mechanisms. *Expert Opin Drug Saf* **5**:157-168.

McKenna KF, Baker GB, Coutts RT and Greenshaw AJ (1992) Chronic administration of the antidepressant-antipanic drug phenelzine and its N-acetylated analogue: effects on monoamine oxidase, biogenic amines, and alpha 2-adrenoreceptor function. *J Pharm Sci* **81**:832-835.

McManus DJ and Greenshaw AJ (1991) Differential effects of chronic antidepressants in behavioural tests of beta-adrenergic and GABAB receptor function. *Psychopharmacology (Berl)* **103**:204-208.

Mercader J, Iffiú-Soltesz Z, Brenachot X, Földi A, Dunkel P, Balogh B, Attané C, Valet P, Mátyus P and Carpéné C (2010) SSAO substrates exhibiting insulin-like effects in adipocytes as a promising treatment option for metabolic disorders. *Future Med Chem* **2**:1735-1749.

Mercader J, Iffiú-Soltész Z, Bour S and Carpéné C (2011) Oral Administration of Semicarbazide Limits Weight Gain together with Inhibition of Fat Deposition and of Primary Amine Oxidase Activity in Adipose Tissue. *J Obes* **2011**:475786.

Minet-Ringuet J, Even PC, Valet P, Carpéné C, Visentin V, Prévot D, Daviaud D, Quignard-Boulange A, Tomé D and de Beaurepaire R (2007) Alterations of lipid metabolism and gene expression in rat adipocytes during chronic olanzapine treatment. *Mol Psychiatry* **12**:562-571.

Morin N, Lizcano JM, Fontana E, Marti L, Smih F, Rouet P, Prévot D, Zorzano A, Unzeta M and Carpéné C (2001) Semicarbazide-sensitive amine oxidase substrates stimulate glucose transport and inhibit lipolysis in human adipocytes. *J Pharmacol Exp Ther* **297**:563-572.

Mustafa AG, Al-Shboul O, Alfaqih MA, Al-Qudah MA and Al-Dwairi AN (2017) Phenelzine reduces the oxidative damage induced by peroxynitrite in plasma lipids and proteins. *Arch Physiol Biochem*:1-6.

Mustafa AG, Alfaqih MA and Al-Shboul O (2018) The 4-hydroxynonenal mediated oxidative damage of blood proteins and lipids involves secondary lipid peroxidation reactions. *Exp Ther Med* **16**:2132-2137.

O'Rourke AM, Wang EY, Miller A, Podar EM, Scheyhing K, Huang L, Kessler C, Gao H, Ton-Nu HT, Macdonald MT, Jones DS and Linnik MD (2008) Anti-inflammatory effects of LJP 1586 [Z-3-fluoro-2-(4-methoxybenzyl)allylamine hydrochloride], an amine-based inhibitor of semicarbazide-sensitive amine oxidase activity. *J Pharmacol Exp Ther* **324**:867-875.

Paetsch PR and Greenshaw AJ (1993) 2-Phenylethylamine-induced changes in catecholamine receptor density: implications for antidepressant drug action. *Neurochem Res* **18**:1015-1022.

Pannecoeck R, Serruys D, Benmeridja L, Delanghe JR, van Geel N, Speeckaert R and Speeckaert MM (2015) Vascular adhesion protein-1: Role in human pathology and application as a biomarker. *Crit Rev Clin Lab Sci* **52**:284-300.

Pawar RS and Grundel E (2017) Overview of regulation of dietary supplements in the USA and issues of adulteration with phenethylamines (PEAs). *Drug Test Anal* **9**:500-517.

Perseghin G, Caumo A, Caloni M, Testolin G and Luzi L (2001) Incorporation of the fasting plasma FFA concentration into QUICKI improves its association with insulin sensitivity in nonobese individuals. *J Clin Endocrinol Metab* **86**:4776-4781.

Prentki M and Madiraju SR (2008) Glycerolipid metabolism and signaling in health and disease. *Endocr Rev* **29**:647-676.

Prévot D, Soltesz Z, Abello V, Wanecq E, Valet P, Unzeta M and Carpéné C (2007) Prolonged treatment with aminoguanidine strongly inhibits adipocyte semicarbazide-sensitive amine oxidase and slightly reduces fat deposition in obese Zucker rats. *Pharmacol Res* **56**:70-79.

Salter-Cid LM, Wang E, O'Rourke AM, Miller A, Gao H, Huang L, Garcia A and Linnik MD (2005) Anti-inflammatory effects of inhibiting the amine oxidase activity of semicarbazide-sensitive amine oxidase. *J Pharmacol Exp Ther* **315**:553-562.

Softic S, Gupta MK, Wang GX, Fujisaka S, O'Neill BT, Rao TN, Willoughby J, Harbison C, Fitzgerald K, Ilkayeva O, Newgard CB, Cohen DE and Kahn CR (2017) Divergent effects of glucose and fructose on hepatic lipogenesis and insulin signaling. *J Clin Invest* **127**:4059-4074.

Song MS, Matveychuk D, MacKenzie EM, Duchcherer M, Mousseau DD and Baker GB (2013) An update on amine oxidase inhibitors: multifaceted drugs. *Prog Neuropsychopharmacol Biol Psychiatry* **44**:118-124.

Sonta T, Inoguchi T, Tsubouchi H, Sekiguchi N, Kobayashi K, Matsumoto S, Utsumi H and Nawata H (2004) Evidence for contribution of vascular NAD(P)H oxidase to increased oxidative stress in animal models of diabetes and obesity. *Free Radic Biol Med* **37**:115-123.

Vachharajani V and Granger DN (2009) Adipose tissue: a motor for the inflammation associated with obesity. *IUBMB Life* **61**:424-430.

Visentin V, Bour S, Boucher J, Prévot D, Valet P, Ordener C, Parini A and Carpéné C (2005) Glucose handling in streptozotocin-induced diabetic rats is improved by tyramine but not by the amine oxidase inhibitor semicarbazide. *Eur J Pharmacol* **522**:139-146.

Wang EY, Gao H, Salter-Cid L, Zhang J, Huang L, Podar EM, Miller A, Zhao J, O'rourke A and Linnik MD (2006) Design, synthesis, and biological evaluation of semicarbazide-sensitive amine oxidase (SSAO) inhibitors with anti-inflammatory activity. *J Med Chem* **49**:2166-2173.

Wang SH, Yu TY, Tsai FC, Weston CJ, Lin MS, Hung CS, Kao HL, Li YI, Solé M, Unzeta M, Chen YL, Chuang LM and Li HY (2018) Inhibition of semicarbazide-sensitive amine oxidase reduces atherosclerosis in apolipoprotein E-deficient mice. *Transl Res* **197**:12-31.

Weston CJ, Shepherd EL, Claridge LC, Rantakari P, Curbishley SM, Tomlinson JW, Hubscher SG, Reynolds GM, Aalto K, Anstee QM, Jalkanen S, Salmi M, Smith DJ, Day CP and Adams DH (2015) Vascular adhesion protein-1 promotes liver inflammation and drives hepatic fibrosis. *J Clin Invest* **125**:501-520.

Yan HJ, Zhou SY, Li Y, Zhang H, Deng CY, Qi H and Li FR (2016) The effects of LSD1 inhibition on self-renewal and differentiation of human induced pluripotent stem cells. *Exp Cell Res* **340**:227-

237.

Zhao Z, Zhang HT, Bootzin E, Millan MJ and O'Donnell JM (2009) Association of changes in norepinephrine and serotonin transporter expression with the long-term behavioral effects of antidepressant drugs. *Neuropsychopharmacology* **34**:1467-1481.

Zhou M and Panchuk-Voloshina N (1997) A one-step fluorometric method for the continuous measurement of monoamine oxidase activity. *Anal Biochem* **253**:169-174.

Zimmermann U, Kraus T, Himmerich H, Schuld A and Pollmächer T (2003) Epidemiology, implications and mechanisms underlying drug-induced weight gain in psychiatric patients. *J Psychiatr Res* **37**:193-220.

Zorzano A, Abella A, Marti L, Carpéné C, Palacín M and Testar X (2003) Semicarbazide-sensitive amine oxidase activity exerts insulin-like effects on glucose metabolism and insulin-signaling pathways in adipose cells. *Biochim Biophys Acta* **1647**:3-9.

Footnotes: This research was funded by the European grant INTERREG IVB SUDOE [Grant 1/P1/E178] "DIOmed Project".

Legends for figures

Figure 1. Effects of chronic phenelzine treatment on body weight and energy efficiency in C57BL/6 male mice. **(A)** Body weight evolution, **(B)** food intake accumulation, **(C)** energy efficiency and **(D)** adiposity index during the 11 weeks of the treatment. Data are mean ± SEM of 12 animals per group, except in the case of food intake which was calculated on a per-cage basis and are the mean ± SEM of 4 cages per group (3 animals/cage). Two-way repeated measures ANOVA followed by a Bonferroni post-hoc test was performed to compare the different effects of treatment and time (***P*<0.01, ****P*<0.001). PHE, treatment effect; T, time effect; and PHExT, interactive effect between treatment and time.

Figure 2. Influence of chronic phenelzine treatment on adipose and hepatic SSAO (semicarbazide-sensitive amine oxidase) and MAO activities in C57BL/6 male mice. **(A)** 0.1 mM benzylamine oxidation and **(B)** 0.5 mM tyramine oxidation in iWAT by SSAO, MAO and SSAO+MAO, **(C)** 0.1 mM benzylamine and **(D)** 0.5 mM tyramine oxidation in liver by SSAO, MAO and SSAO+MAO, and **(E)** mRNA levels of *Aoc3*, *Maoa* and *Maob* in iWAT and **(F)** in liver. Data are mean ± SEM of 9-10 (amine oxidase activities) or 12 (gene expression) animals per group. Student's t-test was used for the analysis (**P*<0.05, ***P*<0.01, ****P*<0.001).

Figure 3. Effects of chronic phenelzine treatment on adipose lipid metabolism in C57BL/6 male mice. **(A)** Gene expression of *Pparg2* (peroxisome proliferator-activated receptor gamma 2), *Srebp1c* (sterol regulatory element-binding protein-1c), *Fas* (fatty acid synthase), *Pepck* (phosphoenolpyruvate carboxykinase) and *Hsl* (hormone-sensitive lipase) in pWAT, iWAT, iBAT and liver. **(B)** Glucose incorporation as a measure of *de novo* lipogenesis in visceral adipocytes when incubated with insulin, Bza (benzylamine), Van (vanadate) and a combination of Bza+Van. **(C)** Basal, Iso (isoprenaline) and Iso+Tyr (tyramine) lipolysis in the adipocytes. Data are mean ± SEM of 5 (lipogenesis) or 8 (lipolysis) animals per group. Student's t-test was used for the analysis (**P*<0.05, ***P*<0.01, ****P*<0.001).

Figure 4. Effects of chronic phenelzine treatment on oxidative stress markers in C57BL/6 male mice. **(A)** Spontaneous release of H_2O_2 by fresh pieces of iWAT, **(B)** MDA (malondialdehyde) levels in plasma and liver, and **(C)** aconitase activity in heart and liver. Data are mean ± SEM of

6 (H_2O_2 release) or 12 (malondialdehyde levels and aconitase activity) animals per group. Student's t-test was used for the analysis (**P*<0.05, ***P*<0.01).

Figure 5. Effects of chronic phenelzine treatment on inflammatory markers on C57BL/6 male mice. **(A)** *Mcp1* (monocyte chemoattractant protein 1), *Cd45* (cluster of differentiation 45), *F4/80*, *Il6*, *Il10* and *Tnf* mRNA levels in pWAT. **(B)** *Mcp1, Cd45, Il6 and Tnf* mRNA levels in iWAT. **(C)** *Il6* and *Tnf* hepatic mRNA levels. Data are mean ± SEM of 12 animals per group. Student's t-test was used for the analysis (**P*<0.05, ***P*<0.01).

Figure 6. Influence of chronic phenelzine treatment on circulating lipid-related parameters and in the expression of a key gene in HDL cholesterol uptake in C57BL/6 male mice. **(A)** Plasma levels of NEFAs (non-esterified fatty acids), glycerol, TG (triacylglycerols), LDL- and HDL-cholesterol. **(B)** Hepatic *Srb1* mRNA levels. Data are mean ± SEM of 12 animals per group. Student's t-test was used for the analysis (**P*<0.05, ***P*<0.01).

Figure 7. Effects of chronic phenelzine treatment on glucose and insulin homeostasis in C57BL/6 male mice. **(A)** Overnight fasted blood glucose and insulin levels. **(B)** HOMA-IR, QUICKI, R-QUICKI and δI/δG scores. **(C)** Glycaemic response in tolerance test. Data are mean ± SEM of 12 animals per group. Student's t-test was used for the analysis (**P*<0.05, ***P*<0.01) and two-way repeated measures ANOVA followed by a Bonferroni post-hoc test were performed to compare the different effects of treatment and time.

Figure 8. Effects of chronic phenelzine treatment on energy expenditure in C57BL/6 male mice. **(A)** Rectal temperature, **(B)** VO_2 (O_2 consumption), **(C)** VCO_2 (CO_2 production), **(D)** RQ (respiratory quotient), **(E)** EE (energy expenditure) and **(F)** locomotor activity. Data are mean ± SEM of 6 animals per group, except for rectal temperature (n=12). Student's t-test and two-way repeated measures ANOVA followed by a Bonferroni post-hoc test were performed to compare the different effects of treatment and time (**P*<0.05). PHE, treatment effect; T, time effect; and PHExT, interactive effect between treatment and time.

JPET Fast Forward. Published on July 3, 2019 as DOI: 10.1124/jpet.119.259895
This article has not been copyedited and formatted. The final version may differ from this version.

Tables

Table 1. Influence of phenelzine chronic treatment on biometric and tissue composition parameters in mice fed a high-fat diet.

Parameter	HFD	HFD + PHE
Adiposomatic index (%)	12.1±0.5	10.8±0.7
iWAT		
Mass (%)	4.46±0.13	3.36±0.26 **
Lipid (mg/pad)	1417±124	929±116 **
Protein (mg/pad)	20.8±2	17.4±1.9
DNA (µg/pad)	142±16	95±7 *
eWAT		
Mass (%)	5.24±0.42	5.35±0.37
Lipid (mg/pad)	1924±128	1727±189
Protein (mg/pad)	25.9±1.8	20.1±1.9 *
DNA (µg/pad)	251±13	200±16 *
iBAT		
Mass (%)	0.51±0.03	0.041±0.03 *
Lipid (mg/pad)	147±14	92±10 **
Protein (mg/pad)	12.8±0.6	12.3±0.5
DNA (µg/pad)	15±0.9	12.8±0.9
pWAT		
Mass (%)	1.85±0.08	1.72±0.11
Liver		
Mass (%)	3.87±0.2	3.73±0.16
Lipid (mg/pad)	274±58	116±28 *
Protein (mg/pad)	290±28	252±15
DNA (µg/pad)	1707±161	1396±175
Skeletal muscle		
Lipid (mg/g tissue)	16.1±1.8	10.7±0.8 *
Heart		
Mass (%)	0.42±0.02	0.41±0.01

Eleven-week-old C57BL/6 male mice on a high-fat diet received water (HFD) or 88.9

µmol phenelzine/kg body weight/day to drink (HFD+PHE) for 11 weeks. WAT, white adipose tissue; pWAT, perirenal WAT; eWAT, epididymal WAT; iWAT, inguinal WAT; iBAT, interscapular brown adipose tissue. Data are the mean ± SEM of n=12/group. A Student's t-test was performed. Difference HFD vs. HFD+PHE mice: * $P < 0.05$; ** $P < 0.01$.

JPET Fast Forward. Published on July 3, 2019 as DOI: 10.1124/jpet.119.259895
This article has not been copyedited and formatted. The final version may differ from this version.

Table 2. Influence of phenelzine chronic treatment on the expression of genes related to oxidative metabolism in mice fed a high-fat diet.

Parameter	HFD	HFD+PHE	*p* value
iBAT			
Cpt1b	100±9	123±8 *	
Ppara	100±11	123±14	
Ppargc1a	100±22	136±27	
Foxc2	100±14	111±15	
Vegf	100±9	125±10	0.061
Ucp1	100±11	119±10	
Liver			
Acc2	100±14	53±9 **	
Ppara	100±9	48±5 ***	
Skeletal muscle			
Cd36	100±25	71±7	
Glut4	100±8	81±3	0.056
Ucp3	100±7	109±15	
Ppargc1a	100±8	84±8	0.056
Ppara	100±12	69±4 **	
Cpt1b	100±7	75±5 **	

Eleven-week-old C57BL/6 male mice on a high-fat diet received water (HFD) or 88.9 µmol phenelzine/kg body weight/day to drink (HFD+PHE) for 11 weeks. Gene expression of *Cpt1b* (carnitine palmitoyltransferase 1B), *Ppara* (peroxisome proliferator activated receptor alpha), *Ppargc1a* (peroxisome proliferator-activated receptor gamma coactivator 1-alpha), *Foxc2* (forkhead box C2), *Vegf* (vascular endothelial growth factor), *Ucp1* (uncoupling protein 1), *Acc2* (acetyl carboxylase 2), *Cd36* (cluster of differentiation 36) *and Glut4* (glucose transporter 4). iBAT, interscapular brown adipose tissue. Data are the mean ± SEM of *n*=12/group. A Student's *t*-test was performed. Difference HFD vs. HFD+PHE mice: * $P < 0.05$; ** $P < 0.01$; *** $P < 0.001$.

JPET Fast Forward. Published on July 3, 2019 as DOI: 10.1124/jpet.119.259895
This article has not been copyedited and formatted. The final version may differ from this version.

Figures

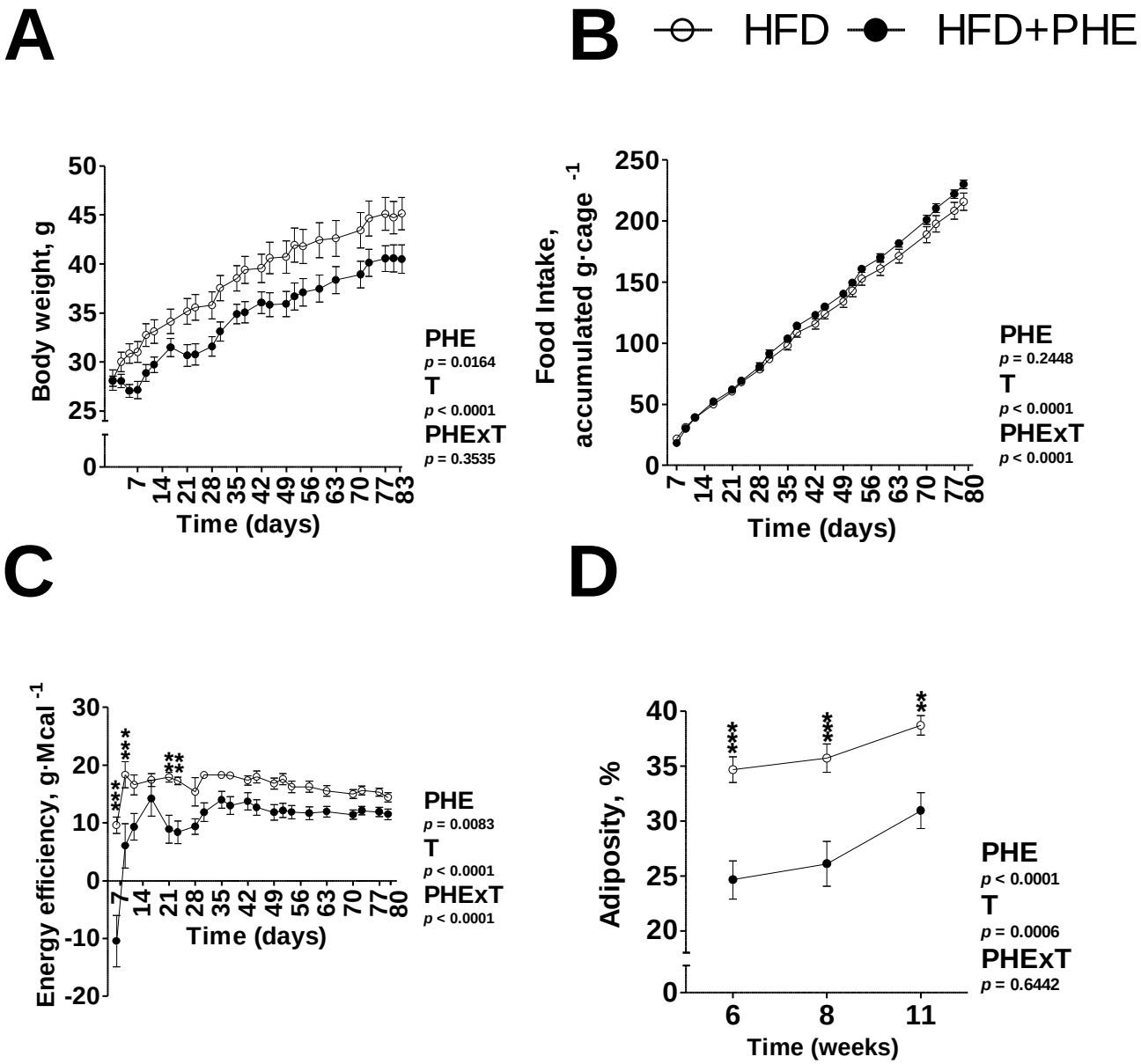

Figure 1

JPET Fast Forward. Published on July 3, 2019 as DOI: 10.1124/jpet.119.259895
This article has not been copyedited and formatted. The final version may differ from this version.

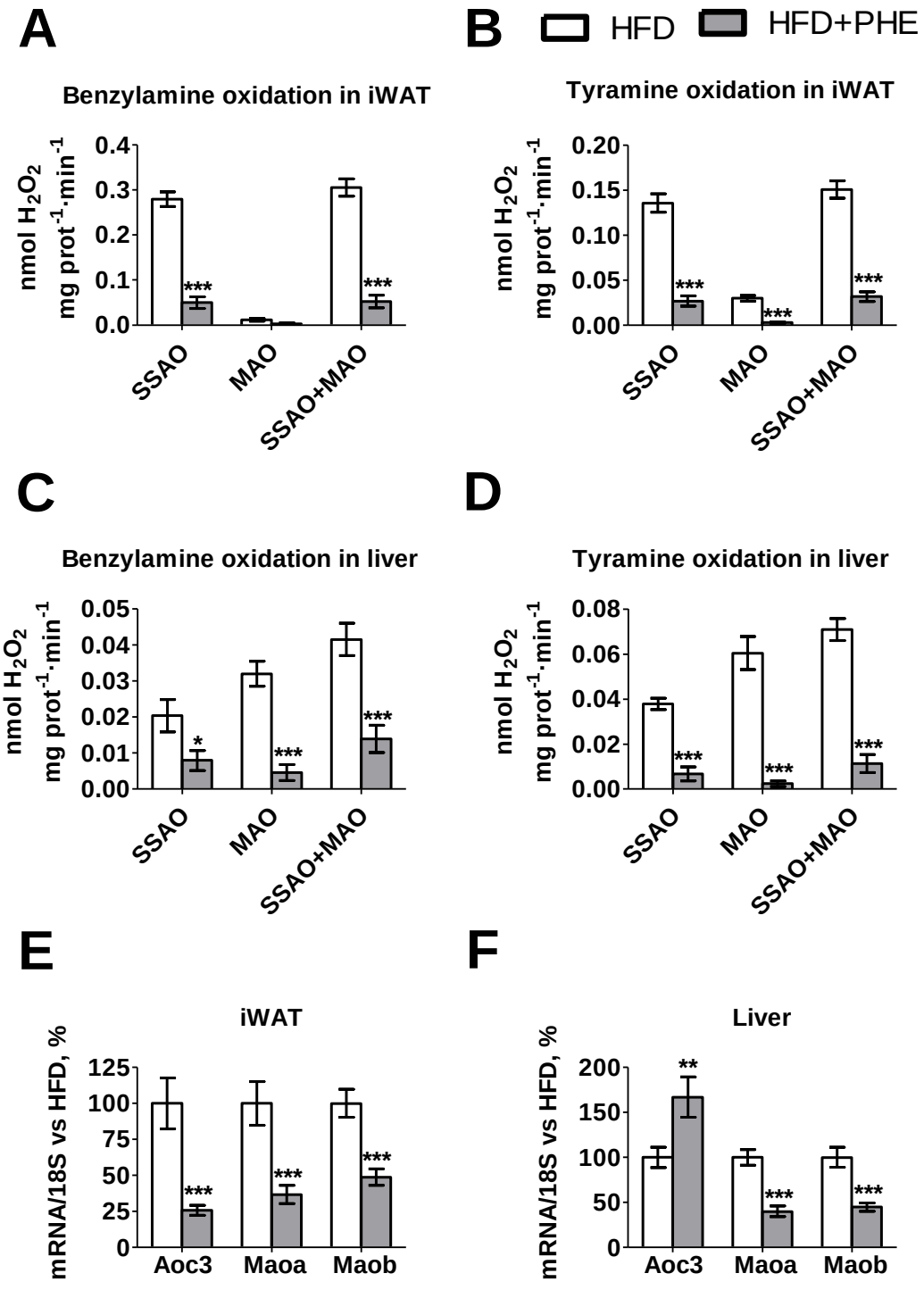

Figure 2

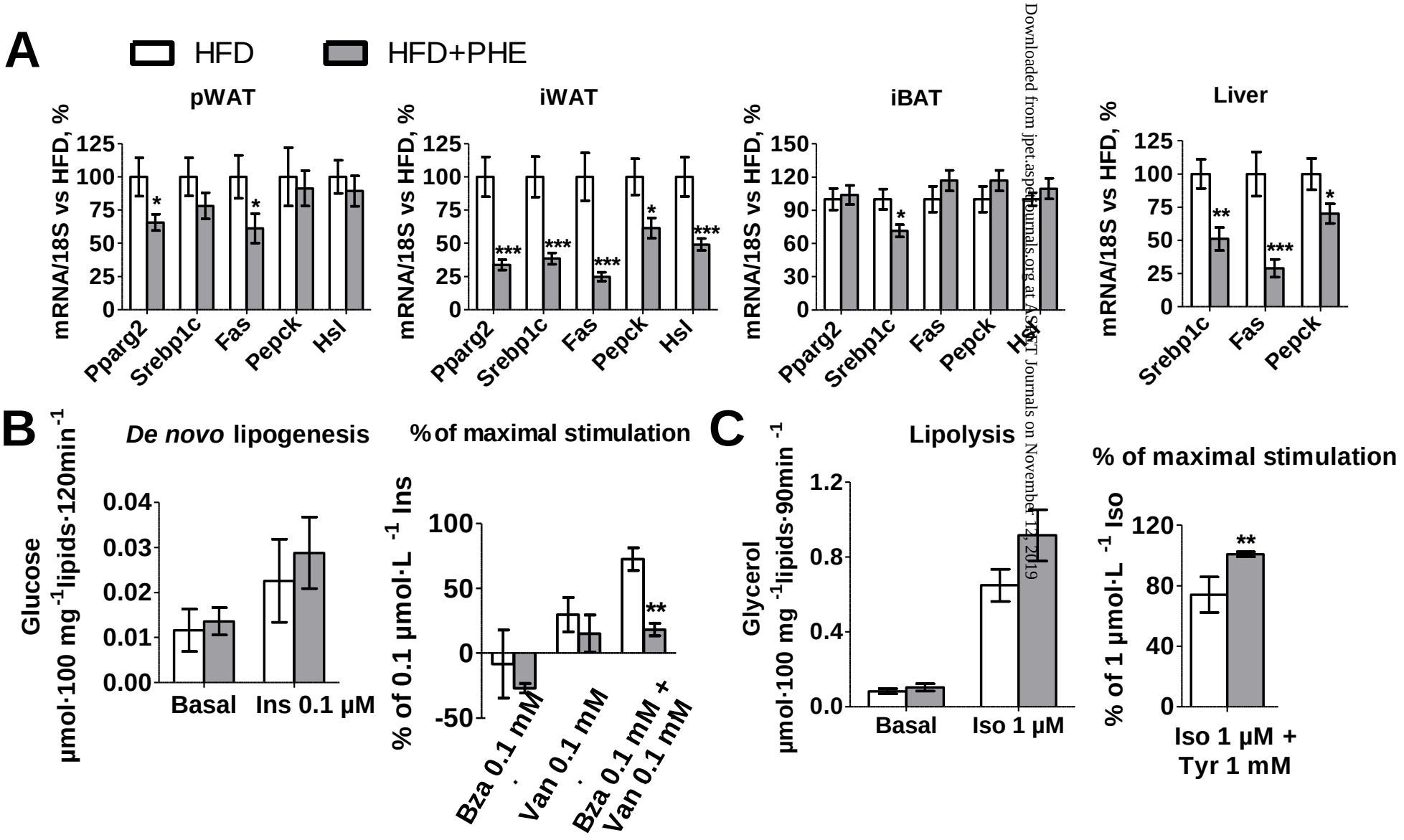

Figure 3

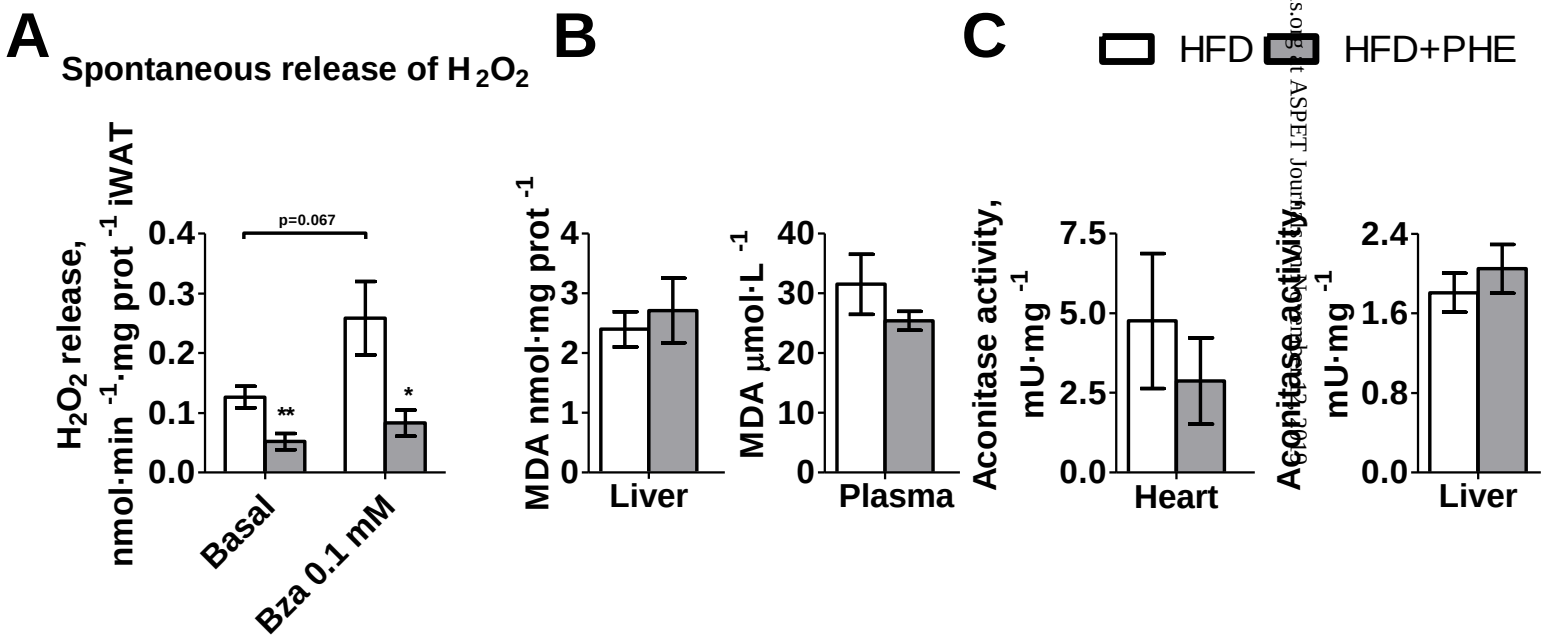

Figure 4

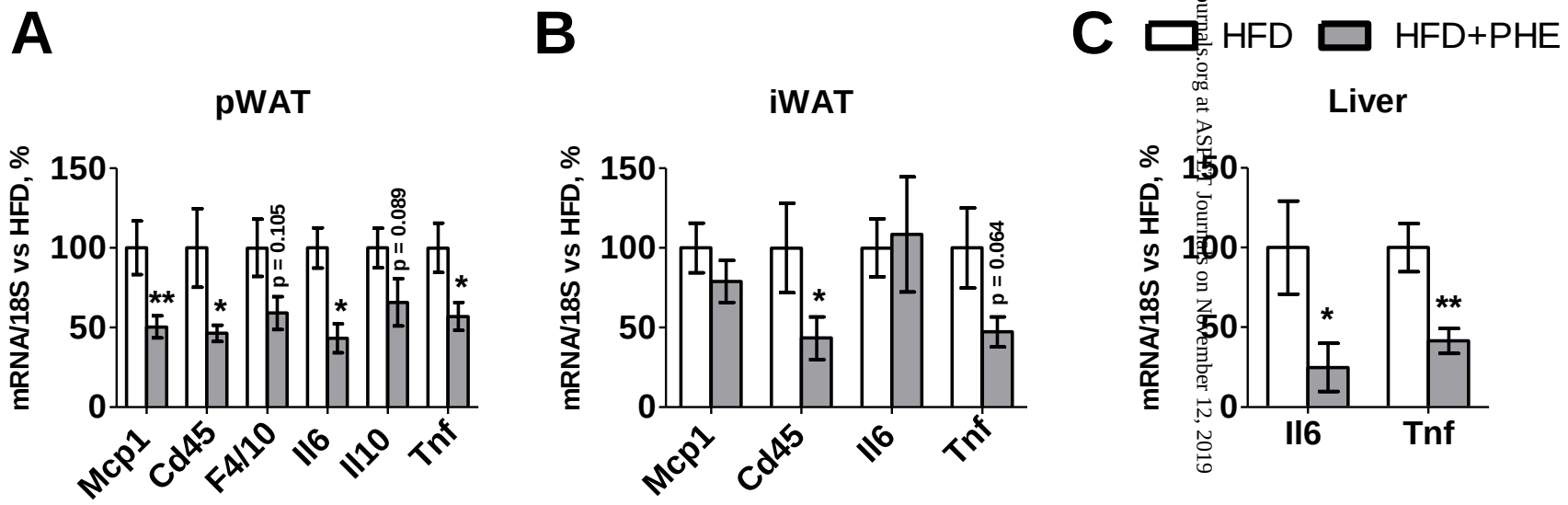

Figure 5

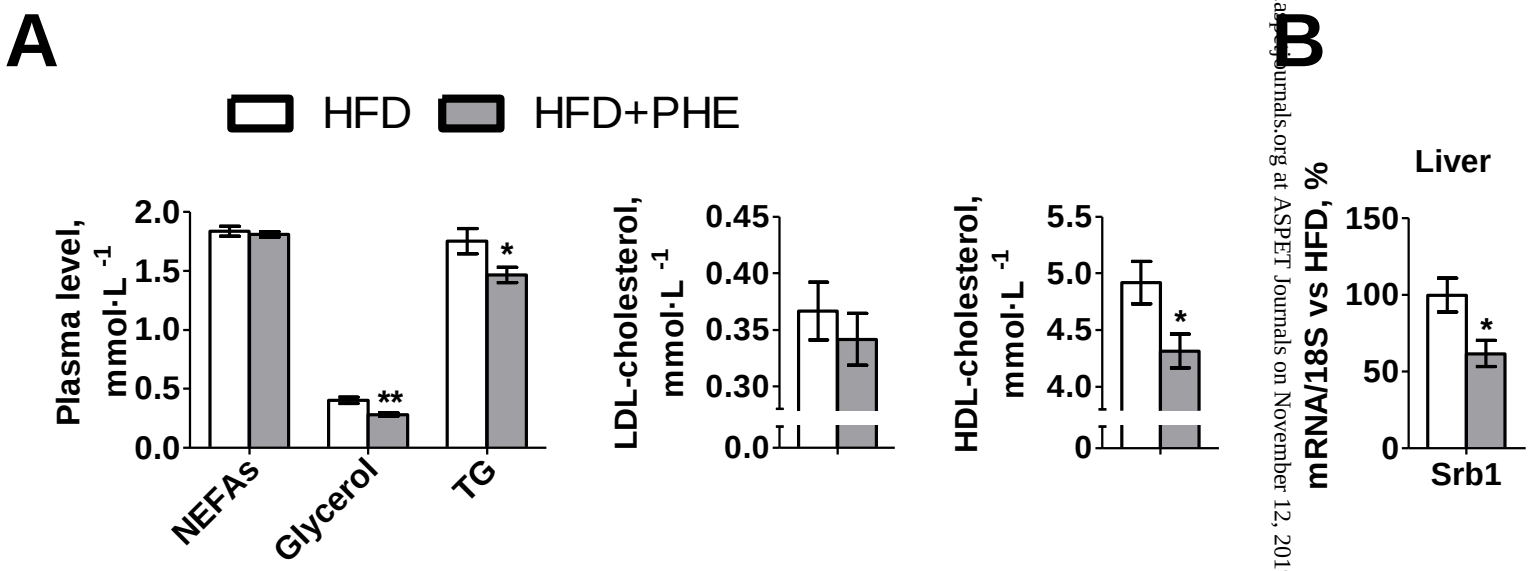

Figure 6

JPET Fast Forward. Published on July 3, 2019 as DOI: 10.1124/jpet.119.259895
This article has not been copyedited and formatted. The final version may differ from this version.

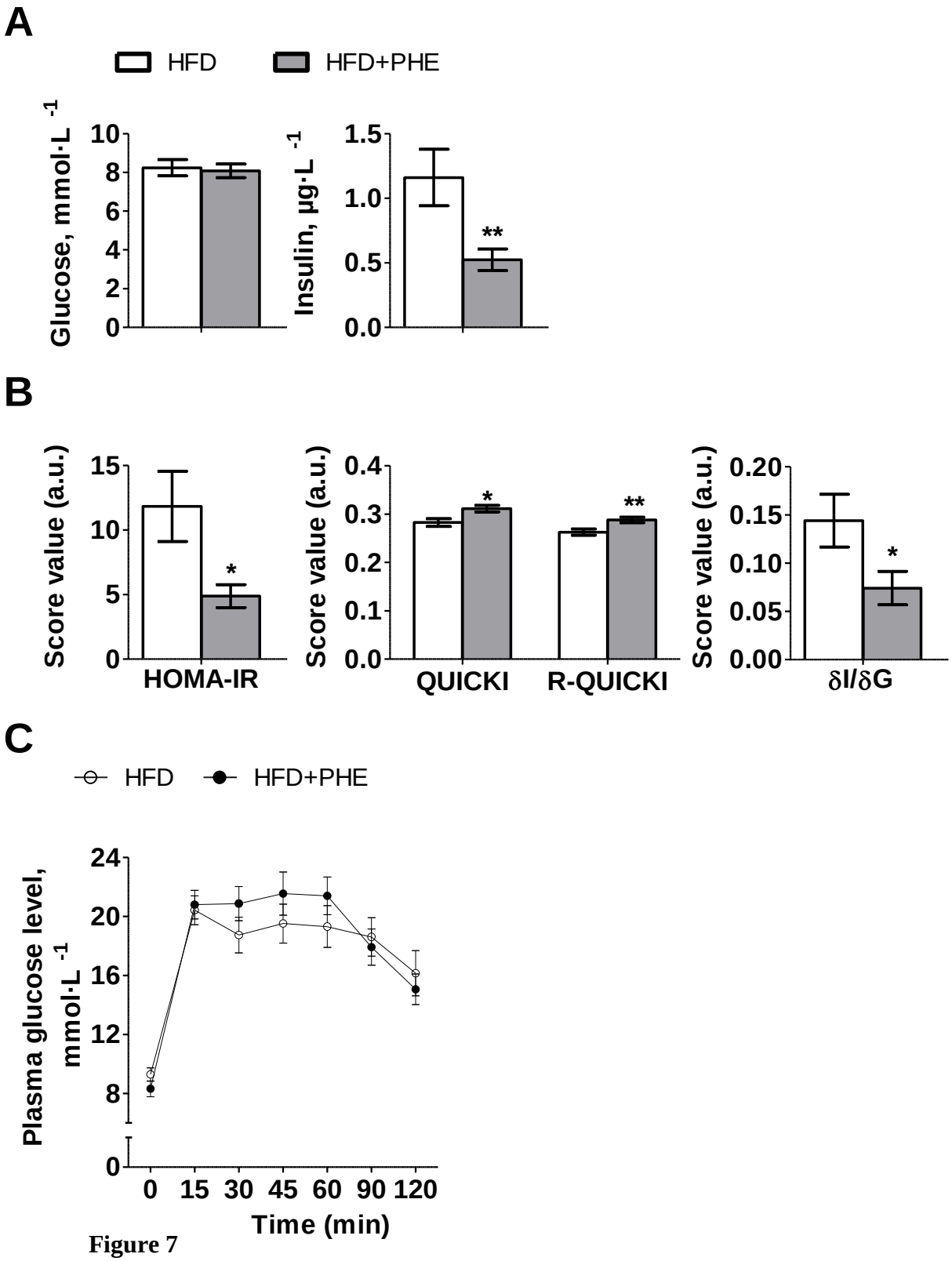

Figure 7

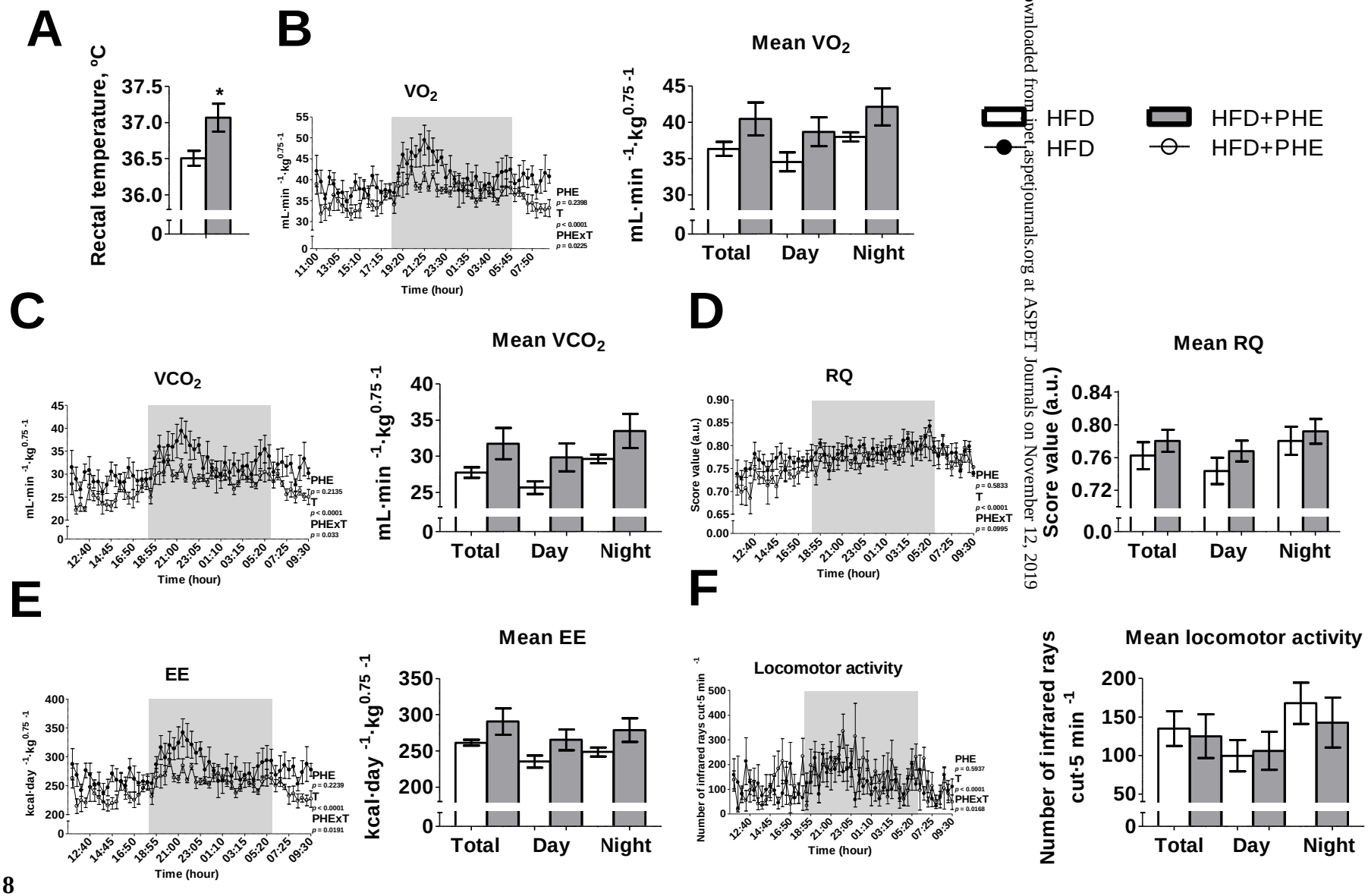

Figure 8